

Article

In Situ DRIFTS Studies of NH₃-SCR Mechanism over V₂O₅-CeO₂/TiO₂-ZrO₂ Catalysts for Selective Catalytic Reduction of NO_x

Yaping Zhang, Xiupeng Yue, Tianjiao Huang, Kai Shen * and Bin Lu

Key Laboratory of Energy Thermal Conversion and Control of Ministry of Education, School of Energy and Environment, Southeast University, Nanjing 210096, China; 101011153@seu.edu.cn (Y.Z.); yuexiupengbg@163.com (X.Y.); 220150460@seu.edu.cn (T.H.); BinLu909@163.com (B.L.)

* Correspondence: shka@263.net; Tel.: +86-25-8379-0667

Received: 19 June 2018; Accepted: 24 July 2018; Published: 28 July 2018



Abstract: TiO₂-ZrO₂ (Ti-Zr) carrier was prepared by a co-precipitation method and 1 wt. % V₂O₅ and 0.2 CeO₂ (the Mole ratio of Ce to Ti-Zr) was impregnated to obtain the V₂O₅-CeO₂/TiO₂-ZrO₂ catalyst for the selective catalytic reduction of NO_x by NH₃. The transient activity tests and the in situ DRIFTS (diffuse reflectance infrared Fourier transform spectroscopy) analyses were employed to explore the NH₃-SCR (selective catalytic reduction) mechanism systematically, and by designing various conditions of single or mixing feeding gas and pre-treatment ways, a possible pathway of NO_x reduction was proposed. It was found that NH₃ exhibited a competitive advantage over NO in its adsorption on the catalyst surface, and could form an active intermediate substance of -NH₂. More acid sites and intermediate reaction species (-NH₂), at lower temperatures, significantly promoted the SCR activity of the V₂O₅-0.2CeO₂/TiO₂-ZrO₂ catalyst. The presence of O₂ could promote the conversion of NO to NO₂, while NO₂ was easier to reduce. The co-existence of NH₃ and O₂ resulted in the NH₃ adsorption strength being lower, as compared to tests without O₂, since O₂ could occupy a part of the active site. Due to CeO₂'s excellent oxygen storage-release capacity, NH₃ adsorption was weakened, in comparison to the 1 wt. % V₂O₅-0.2CeO₂/TiO₂-ZrO₂ catalyst. If NO_x were to be pre-adsorbed in the catalyst, the formation of nitrate and nitro species would be difficult to desorb, which would greatly hinder the SCR reaction. All the findings concluded that NH₃-SCR worked mainly through the Eley-Rideal (E-R) mechanism.

Keywords: in situ DRIFTS; V₂O₅-CeO₂/TiO₂-ZrO₂; catalysts; NH₃-SCR mechanism; NO_x; adsorption

1. Introduction

Generally, nitrogen oxides (NO_x), which may cause environmental problems, such as: Photochemical smog; acid rain; ozone depletion; and, health hazards, are mainly emitted from the industrial combustion of fossil fuels. Therefore, the reduction of NO_x has become an important research field for atmospheric environmental control. Currently, the selective catalytic reduction (SCR) is the most promising method to reduce the emissions of NO_x [1,2]. The temperature window of the traditional V-W (Mo)/Ti catalyst is 300–400 °C, but in some coal-fired power plants, the temperature of exhaust gas is lower. In order to enhance the NO_x conversion rate, the exhaust gases were reheated, which caused a large waste of energy. The narrow temperature window restrained its application. Thus, many researchers redirected their study to focus on the catalyst, which has superior low-temperature activity.

The VO_x/TiO₂ system for SCR has been studied extensively in the past and a number of reaction mechanisms have been proposed. It is generally accepted that the Brønsted and Lewis

acid sites are essential for the reaction mechanism. Topsoe et al. [3] proposed a “Brønsted NH_4^+ ” mechanism over a V_2O_5 -based catalyst, which has gained the majority of support in the literature. Arnarson et al. [4] observed the SCR reaction over the $\text{VO}_3\text{H}/\text{TiO}_2$ catalyst and demonstrated that the Brønsted acid site served to capture the NH_3 and increased the NH_4^+ stability (increased Brønsted acid strength), which impacted the catalytic rate in a negative direction. Marberger et al. [5] had a similar conclusion for the $\text{V}_2\text{O}_5\text{-WO}_3/\text{TiO}_2$ catalyst. That is, the Brønsted acid sites hardly contributed to the SCR activity and mainly served as an NH_3 pool to replenish the Lewis sites. NO reacted predominantly with NH_3 adsorbed in the Lewis acid sites at low temperatures. SCR reactions over Ce-based catalysts mainly followed two mechanisms, one is the Eley–Rideal mechanism (i.e., the reaction of gaseous NO with adsorbed NH_3 species), and the other is the Langmuir–Hinshelwood mechanism (i.e., the reaction of adsorbed NO_x with adsorbed NH_3 species on adjacent sites) [6]. While these two reaction pathways probably do not exclude each other, it is essential to understand whether either or both species are relevant. Vuong et al. [7] reported that NH_3 -SCR proceeded from a Langmuir–Hinshelwood mechanism on bare supports (TiO_2), while an Eley–Rideal mechanism operated on V-containing catalysts.

In recent years, cerium oxides have attracted extensive attention due to their outstanding oxygen storage-release capacity and excellent redox properties in the low-temperature NH_3 -SCR reactions [8–10]. In $\text{V}/\text{Ce}_{1-x}\text{Ti}_x\text{O}_2$ catalysts, Ce-O sites are effectively covered by VO_x species, which hinder the formation of surface nitrates and cause the switch in the reaction mechanism. Zhang et al. [11] observed the adsorption and reaction processes in DRIFTS (diffuse reflectance infrared Fourier transform spectroscopy) spectra and concluded that the $\text{cis-N}_2\text{O}_2^{2-}$ formed on CeO_2 reacted more favorably with NH_3 than with other nitrate species. Galvez et al. [12] demonstrated that the SCR reaction over activated carbon supported the V_2O_5 catalysts ($\text{V}_2\text{O}_5/\text{AC}$) that took place between the adsorbed species of NH_3 on the Brønsted acid sites, and the NO molecules in the gaseous phase, following an Eley–Rideal (E–R) mechanism. In Yu et al. [13], the study proposed that the SCR reaction over $\text{Zr}_3(\text{PO}_4)_2/\text{CeO}_2\text{-ZrO}_2$ proceeded via the combination of the adjacent, surface N_xO_y species, and the ads- NH_3 species by Langmuir–Hinshelwood (L-H) mechanism. Ma et al. [14] also observed the enhanced NH_3 activation and NO_3 -formation. The latter promoted the reaction of ads- NH_3 and ads- NO_3 -species for the SCR reaction over $\text{Nb}_5\text{O}_x/\text{CeO}_2\text{-ZrO}_2$ catalysts—according to the “L-H” mechanism. Getting to know the reaction pathway and proposing reaction mechanisms is helpful in guiding the design and preparation of the catalysts [15].

In our previous study [9,16], a series of 1 wt. % $\text{V}_2\text{O}_5\text{-CeO}_2/\text{TiO}_2\text{-ZrO}_2$ catalysts with different contents of CeO_2 were prepared by an impregnation method. It was found that the sample of $\text{Ce}/\text{Ti} = 0.2$ (the molar ratio) exhibited a favorable performance with a 92% NO_x conversion rate at 250 °C. In addition, the effect of Ce modification on microscopic properties and the catalytic performance of $\text{V}_2\text{O}_5/\text{TiO}_2\text{-ZrO}_2$ were investigated in more detail. It concluded that the promotional effect of adding Ce mainly laid in the intensified interaction between the metal oxide components and the larger amount of Brønsted and Lewis acid sites, as well as the formation of active intermediates ($-\text{NH}_2$). In this study, we further investigated the NH_3 -SCR mechanism over the optimal 1 wt. % $\text{V}_2\text{O}_5\text{-0.2CeO}_2/\text{TiO}_2\text{-ZrO}_2$ catalyst, and by carrying out transient activity tests and in situ DRIFTS analyses under various conditions of single or mixing feeding gas and pre-treatment ways, proposed a possible reaction pathway.

2. Results and Discussion

2.1. Adsorption and Desorption Properties of NO_x and NH_3 on the Catalysts

The adsorption-desorption behavior of the catalyst is considered to be a crucial step to a heterogeneous catalysis system. To study the desorption status of the reactant gas on the catalyst surface, the desorption of NO on 1 wt. % $\text{V}_2\text{O}_5\text{-0.2CeO}_2/\text{TiO}_2\text{-ZrO}_2$ was studied. As shown in Figure 1, the band at 3670 cm^{-1} was attributed to O-H, and it decreased with the increased temperature until the

negative peak appeared. The band at 3203 cm^{-1} was the result of the hydroxyl vibration. The catalysts contained a little bit of water at a normal temperature, and the water evaporated as the temperature rose; adsorption bands then disappeared. The bands (1618 cm^{-1} , $1367\text{--}1378\text{ cm}^{-1}$, $1245\text{--}1288\text{ cm}^{-1}$, 1130 cm^{-1} , and 1058 cm^{-1}) were ascribed to the adsorbed NO_x , especially the band of 1618 cm^{-1} which was related to weak adsorption of NO and NO_2 [16–18]. In the case of $\text{cis-N}_2\text{O}_2^{2-}$, bands should appear in the $1300\text{--}1400\text{ cm}^{-1}$ [19]. When the temperature exceeded $200\text{ }^\circ\text{C}$, $\text{N}_2\text{O}_2^{2-}$ appeared in the region of $1367\text{--}1378\text{ cm}^{-1}$ and the intensity of peaks increased as the temperature rose. This confirmed that it could exist stably on the surface of the catalyst. The band at 1245 cm^{-1} was due to bridging nitrate; the adsorption intensity receded as the temperature rose, and the band region moved to 1288 cm^{-1} with the generation of monodentate nitrate [17,20,21]. Subsequently, this peak disappeared as the temperature reached $400\text{ }^\circ\text{C}$. The band at 1130 cm^{-1} was assigned to nitrosyl NO^- , which could be oxidized to nitrite and nitrate with the existence of oxygen, and it sharply decreased as the temperature increased [22,23]. The band at 1054 cm^{-1} corresponded to nitrate species, which could exist on the surface of the catalyst stably and was hard to desorb even when the temperature was raised.

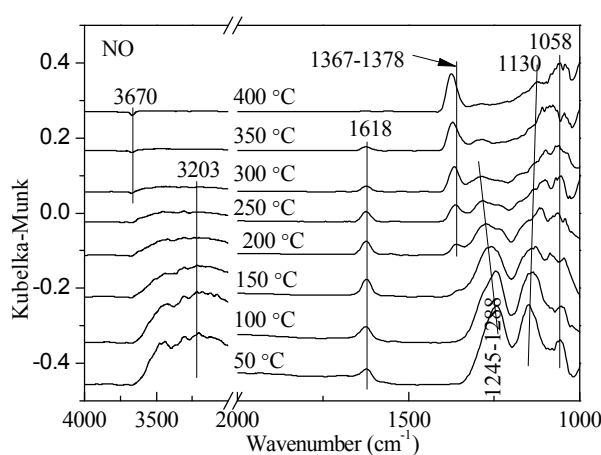


Figure 1. In situ DRIFTS (diffuse reflectance infrared Fourier transform spectroscopy) spectra of NO desorption on 1 wt. % $\text{V}_2\text{O}_5\text{-}0.2\text{CeO}_2/\text{TiO}_2\text{-ZrO}_2$ as a function of temperature after the catalyst was exposed to a flow of 800 ppm NO for 60 min at $25\text{ }^\circ\text{C}$.

As shown in Figure 2a, as N_2 was steadily purged on, it was clear that the adsorption of NO was very weak at $250\text{ }^\circ\text{C}$, and $\text{N}_2\text{O}_2^{2-}$ and nitrate species only appeared at the band of 1371 cm^{-1} and 1052 cm^{-1} . In addition, there was no significant change in peak intensity by increasing the adsorption and desorption time, indicating that it could exist stably on the surface of the catalyst. As shown in Figure 2b, it was observed that the presence of O_2 obviously strengthened the adsorption intensity of NO_x on the surface of catalysts. After being exposed to $\text{NO} + \text{O}_2$ for 60 min, weak adsorption of NO and NO_2 appeared at the band of 1630 cm^{-1} . The bands at 1365 cm^{-1} and 1108 cm^{-1} could be assigned to *cis*- and *trans*- $\text{N}_2\text{O}_2^{2-}$ [19,24], respectively. Simultaneously, the bands at 1284 cm^{-1} and 1038 cm^{-1} were attributed to monodentate nitrate and nitrate species, respectively.

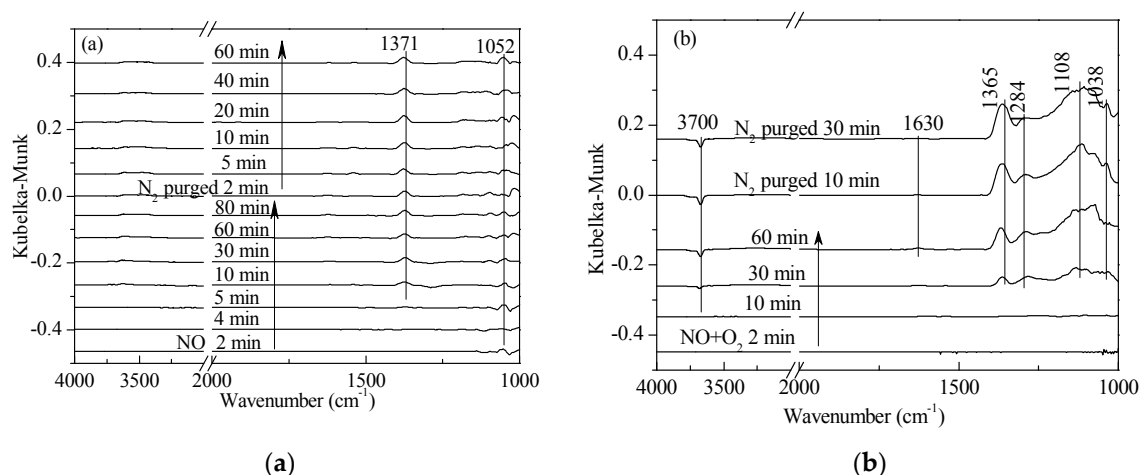


Figure 2. In situ DRIFTS spectra of (a) NO adsorption and (b) NO + O₂ adsorption on 1 wt. % V₂O₅-0.2CeO₂/TiO₂-ZrO₂ catalysts with N₂ purging for various time at 250 °C after the catalysts were exposed to a flow of 800 ppm NO or 800 ppm NO + 5% O₂ for 60 min.

As shown in Figure 3, the adsorption peaks of free O-H appeared at 3662 cm⁻¹ and 3700 cm⁻¹, and the band at 3100–3400 cm⁻¹ was associated with the N-H stretching vibrations, which are linked to Lewis acid sites. The peaks at 1556 cm⁻¹, 1548 cm⁻¹, and 1505 cm⁻¹ corresponded to the formation of intermediate species (-NH₂) in SCR reactions [21]. In addition, there was no significant change in peak intensity as adsorption and desorption time increased. According to our previous study [16], intermediate species (-NH₂) were detected above 300 °C over the V₂O₅/TiO₂-ZrO₂ catalyst. The V₂O₅-0.2CeO₂/TiO₂-ZrO₂ catalyst exhibited more -NH₂ at lower temperatures, which explained its higher activity in comparison to other catalysts. Vuong et al. [11] collected different DRIFTS spectra of bare supports (CeO₂, TiO₂ and CeO₂-TiO₂) and supported vanadium catalysts (V/CeO₂, V/CeO₂-TiO₂ and V/TiO₂) at 200 °C. They reported additional bands at 1510–1520 cm⁻¹ of NH₂, which were only observed on pure CeO₂ and CeO₂-TiO₂. It could be speculated that the addition of Ce was the key factor to affect the surface adsorbed NH₃ species. At the same time, the peaks at 1605 cm⁻¹, 1357 cm⁻¹, 1321 cm⁻¹, 1282 cm⁻¹, 1180 cm⁻¹, and 1133 cm⁻¹ were associated with NH₃ cooperating vibration—linked to Lewis acid sites [25,26]. According to our previous study [16], with the addition of Ce, the acid sites of the catalysts increased and the optimal V₂O₅-0.2CeO₂/TiO₂-ZrO₂ sample possessed the largest amount of surface acid sites, which greatly promoted the SCR reaction. The same trend was observed in Vuong et al. [7]. They demonstrated that the relative amount of Lewis acid sites in the V-containing catalysts decreased in the order V/Ce_{0.5}Ti_{0.5}O₂ > V/CeO₂ > V/TiO₂. The band at 1180 cm⁻¹ in Figure 3a split into two NH₃ adsorption peaks (1085 cm⁻¹ and 1044 cm⁻¹), and the band at 1133 cm⁻¹ in Figure 3b corresponded to the peak at 1085 cm⁻¹. The band at 1678 cm⁻¹ was associated with NH₄⁺ symmetric vibration and is linked to Brønsted acid sites [27,28]. Comparing Figure 3a with Figure 3b, it can be found that the presence of O₂ hindered the adsorption of NH₃. However, in Figure 3b, after the feeding of NH₃ + O₂ was stopped, the intensity of the NH₃ adsorption peak, linked to Lewis acid sites, was stronger than in Figure 3a. It might have been caused by the re-adsorption of desorbed ammonia or weak ammonia adsorption on Lewis acid sites, because CeO₂ had the capacity of oxygen storage-release and O₂ occupied some active sites.

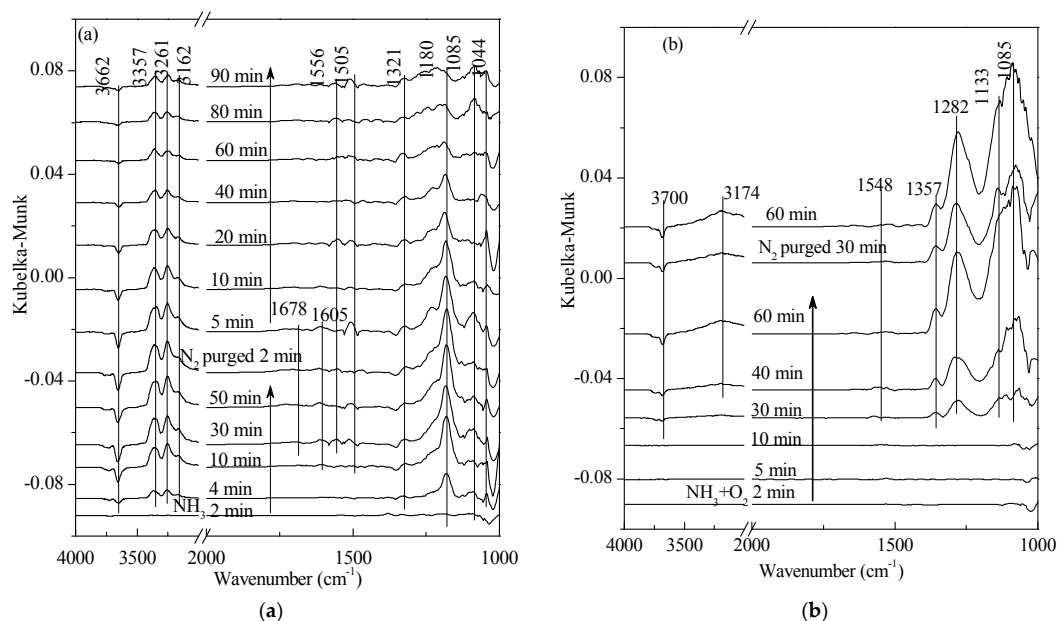


Figure 3. In situ DRIFTS spectra of (a) NH_3 adsorption and (b) $\text{NH}_3 + \text{O}_2$ adsorption on $\text{V}_2\text{O}_5\text{-}0.2\text{CeO}_2/\text{TiO}_2\text{-ZrO}_2$ catalysts with N_2 purging for various time at 250°C after the catalysts were exposed to a flow of 800 ppm NH_3 or 800 ppm $\text{NH}_3 + 5\% \text{O}_2$ for 60 min.

2.2. Transient Response Experiment Analysis

In order to illuminate the difference between NO_x species and explain the SCR reaction mechanism, transient reaction studies by in situ DRIFTS spectra were performed. As shown in Figure 4, the NH_3 adsorption peak could be found after NH_3 and NO were introduced for two min. After adsorption was saturated, the bands at 3400 cm^{-1} , 3100 cm^{-1} , and 1198 cm^{-1} were associated with NH_3 adsorption and was linked to Lewis acid sites. The intermediate species ($-\text{NH}_2$) appeared at 1591 cm^{-1} , which implied more active intermediates for the NH_3 oxidation reaction. No obvious NO_x adsorption was observed; it was a preliminary inference that SCR reactions mainly followed from the Eley–Rideal mechanism.

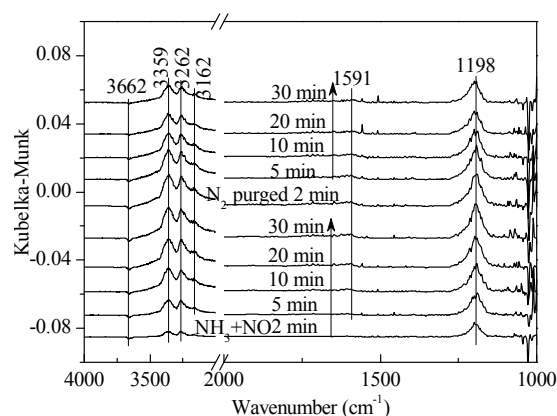


Figure 4. In situ DRIFTS spectra of $\text{NH}_3 + \text{NO}$ adsorption on 1 wt. % $\text{V}_2\text{O}_5\text{-}0.2\text{CeO}_2/\text{TiO}_2\text{-ZrO}_2$ catalysts with N_2 purging for various times at 250°C after the catalysts were exposed to a flow of 800 ppm NH_3 and 800 ppm NO for 60 min.

As shown in Figure 5, catalysts were exposed to the flow of NO and $\text{NO} + \text{O}_2$ at 250°C for 60 min. The O-H adsorption peaks appeared at 3510 cm^{-1} and 3528 cm^{-1} . The N-H stretching vibration

peaks appeared in the range of 3400–3100 cm^{-1} after NO was introduced for two min. However, in Figure 5b, NH_3 adsorption peaks appeared after NH_3 was introduced for 10 min in the same region. NO_2 asymmetric vibration adsorption peaks appeared at 1610 cm^{-1} and 1620 cm^{-1} in Figure 5a,b, respectively. The bands at 1583 cm^{-1} , 1226 cm^{-1} , and 1231 cm^{-1} were ascribed to bridging nitrates. $\text{cis-N}_2\text{O}_2^{2-}$ appeared at 1353 cm^{-1} in Figure 5b, and it shifted to the region of 1335 cm^{-1} with the introduction of NH_3 , which then weakened the adsorption. When introducing $\text{NO} + \text{O}_2$ again, the adsorption peak recovered to 1353 cm^{-1} .

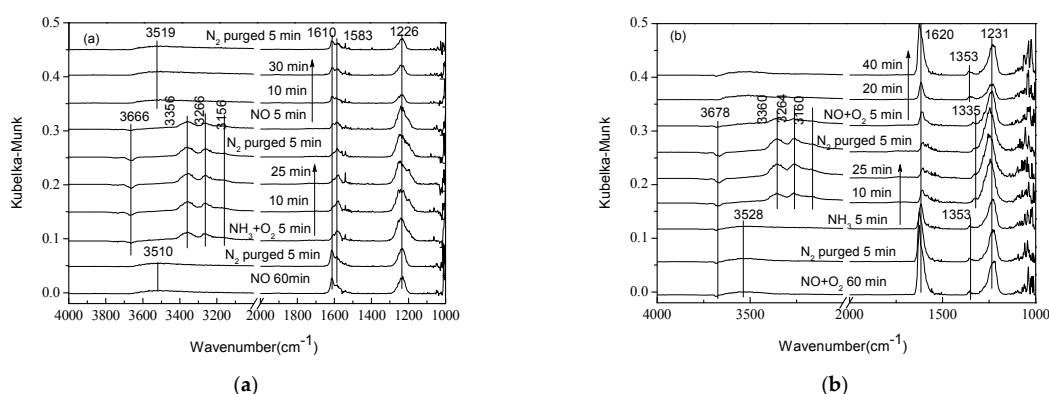


Figure 5. In situ DRIFTS spectra of the transient reactions at 250 °C between (a) NO and pre-adsorbed $\text{NH}_3 + \text{O}_2$ and (b) NH_3 , and pre-adsorbed $\text{NO} + \text{O}_2$ species over 1 wt. % $\text{V}_2\text{O}_5\text{-}0.2\text{CeO}_2/\text{TiO}_2\text{-ZrO}_2$ catalysts recorded as a function of time.

NH_3 had no obvious influence on the NO_x adsorption peak at 2000–1000 cm^{-1} , especially after being exposed to $\text{NO} + \text{O}_2$ where the influence became tinier. After the pre-adsorption of NO, the intensity of the NO_x adsorption peak was obvious, but NH_3 adsorption could barely be found. With the introduction of NH_3 , the N-H stretching vibration was present in the range of 3400–3100 cm^{-1} , as seen in both Figure 5a,b. The results showed that when $\text{NO} + \text{O}_2$ was injected separately, $\text{NO} + \text{O}_2$ occupies SCR active reaction sites and restrains the adsorption of NH_3 , before hindering the SCR reaction. When NO and $\text{NO} + \text{O}_2$ was reintroduced, respectively, peaks located at 3519 cm^{-1} and assigned to O-H adsorption were observed. The intensity of the NO_x adsorption peak had no decrement; on the contrary, NH_3 adsorption, which was linked to Lewis acid sites, disappeared. These results indicated that the gas-phase NO_x had reacted with NH_3 on Lewis acid sites, which verified the Eley–Rideal mechanism on catalysts. However, in Chen et al. [29], a Langmuir–Hinshelwood mechanism operated on the CeTi catalyst, and adsorbed NH_3 and NH_4^+ that reacted with NO/O_2 from the gas phase. Vuong et al. [7] demonstrated that the switch in reaction mechanisms has its roots in the structural differences of catalysts and supports. In $\text{V}/\text{Ce}_{1-x}\text{Ti}_x\text{O}_2$ catalysts, Ce-O sites are effectively covered by VO_x species, which hinders the formation of surface nitrates and causes the switch in the reaction mechanism.

As shown in Figure 6a, when $\text{NO} + \text{O}_2$ is introduced, the adsorption peaks at the region of 3400–3100 cm^{-1} and 1189 cm^{-1} disappeared, while the O-H adsorption peak (1618 cm^{-1}), the $\text{N}_2\text{O}_2^{2-}$ adsorption peak (1371 cm^{-1} and 1112 cm^{-1}), and the nitrate species peak (1024 cm^{-1}) appeared. When NH_3 was introduced again, the NO_2 adsorption peak disappeared. Moreover, a strong adsorption of NH_3 appeared at the region of 3400–3100 cm^{-1} and 1259 cm^{-1} . Brønsted acid adsorption appeared at 1698 cm^{-1} and 1428 cm^{-1} and considerably intensified, while other NO_x adsorption had no obvious change.

As shown in Figure 6b, NO was introduced after being exposed to $\text{NH}_3 + \text{O}_2$. Bridging nitrate and monodentate nitrate appeared at 1575 cm^{-1} and O-H vibration appeared at 3566 cm^{-1} . When $\text{NH}_3 + \text{O}_2$ were introduced again, the O-H vibration became stronger and the NH_3 adsorption peak at the region of 3400–3100 cm^{-1} was heavily weakened, as compared with that in Figure 6a. As a result, it can be concluded that O_2 reacted with NO first.

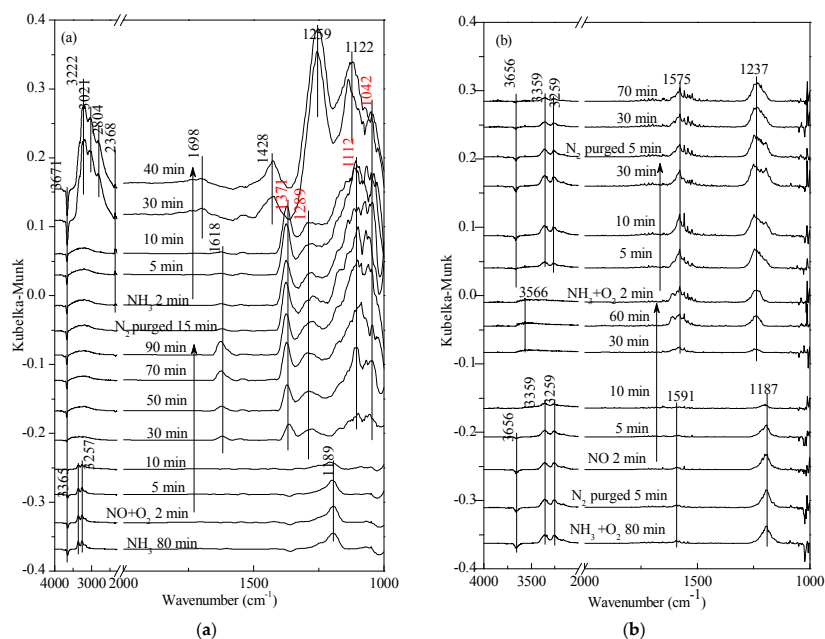


Figure 6. In situ DRIFTS spectra of the transient reactions at 250 °C between (a) NO + O₂ and pre-adsorbed NH₃, and (b) NO and pre-adsorbed NH₃ + O₂ species over 1 wt. % V₂O₅-0.2CeO₂/TiO₂-ZrO₂ catalysts recorded as a function of time.

In Figure 7, NH₃ was introduced first, and then NO was introduced in combination with NH₃. Lastly, O₂ was also introduced with NH₃, NO, and O₂ being presented at the same time. In these three different atmospheres, the intensity of NH₃ adsorption on Lewis acid sites had no change. Meanwhile, the active intermediate species of -NH₂ appeared at 1588 cm⁻¹, indicating that NH₃ molecules continued to be adsorbed on the catalytic surface with the process of reaction. The stable existence of intermediate species (-NH₂) explained the high SCR activity of the V₂O₅-0.2CeO₂/TiO₂-ZrO₂ catalyst at low temperatures. Simultaneously, the intensity of the O-H negative peak receded gradually, which might have been caused by the H₂O produced in the SCR reaction.

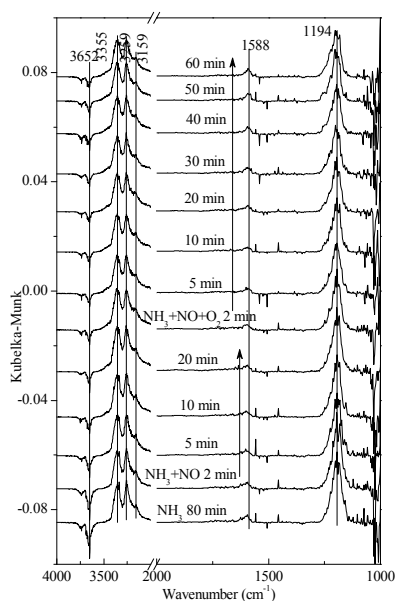


Figure 7. In situ DRIFTS spectra of NH₃ + NO + O₂ pre-adsorption transient reaction at 250 °C over 1 wt. % V₂O₅-0.2CeO₂/TiO₂-ZrO₂ catalysts recorded as a function of time.

2.3. Steady-State Response Experiments

As shown in Figure 8, catalysts were saturated at 25 °C after 60 min pre-adsorption. -NO_2 adsorption appeared at 1839 cm^{-1} and 1843 cm^{-1} . The bands at 1692 cm^{-1} , 1682 cm^{-1} , 1443 cm^{-1} , and 1419 cm^{-1} were associated with NH_4^+ adsorption, linked to Brønsted acid sites, and the bands of $3400\text{--}3100\text{ cm}^{-1}$, 1197 cm^{-1} , and 1215 cm^{-1} were associated with NH_3 adsorption, linked to Lewis acid sites. As shown in Figure 8b, $\text{N}_2\text{O}_2^{2-}$ species appeared at 1106 cm^{-1} with the presence of O_2 , which indicated that the existence of O_2 would promote NO adsorption. Comparing Figure 8a with Figure 8b, NH_3 adsorption became much stronger with the existence of O_2 . At the same time, the combination of NO_x and NH_3 appeared at 1248 cm^{-1} , and $\text{N}_2\text{O}_2^{2-}$ species decreased with increasing temperatures, indicating that O_2 is essential for SCR reactions.

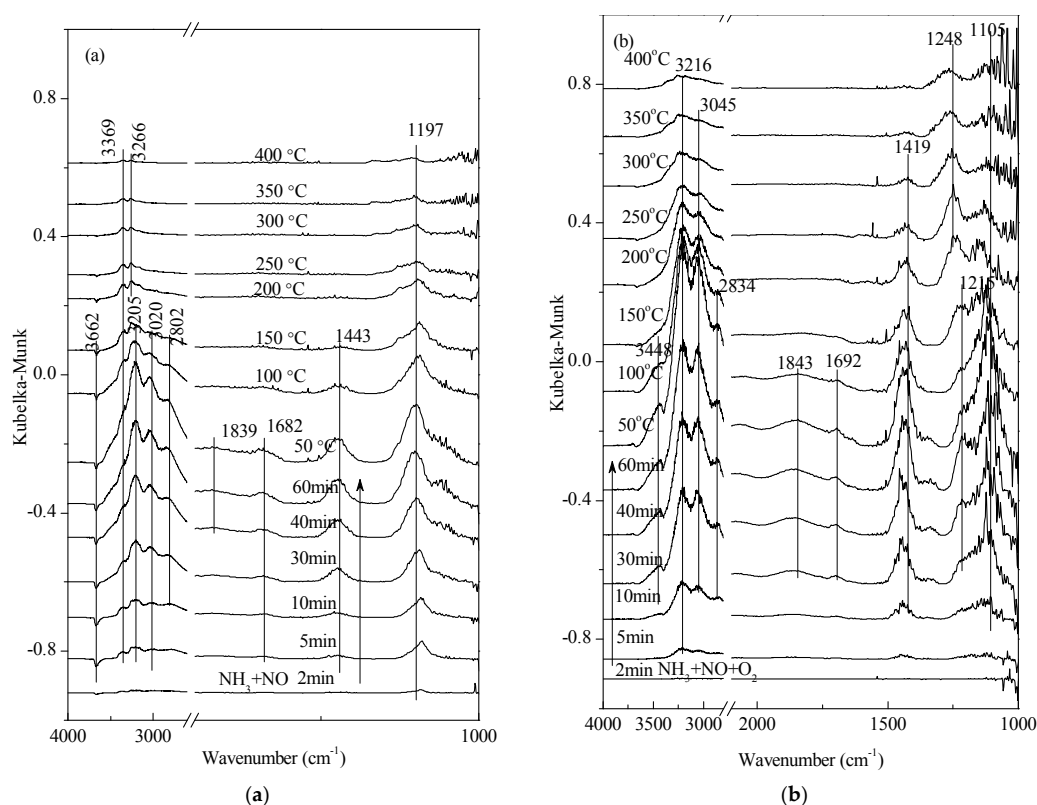


Figure 8. In situ DRIFTS spectra of (a) $\text{NH}_3 + \text{NO}$ desorption and (b) $\text{NH}_3 + \text{NO} + \text{O}_2$ desorption on 1 wt. % $\text{V}_2\text{O}_5\text{-}0.2\text{CeO}_2/\text{TiO}_2\text{-ZrO}_2$ as a function of temperature after the catalyst was exposed to a flow of 800 ppm NO , 800 ppm NH_3 , and 5% O_2 for 60 min at 25 °C.

2.4. Transient SCR Activity Test Experiments

As shown in Figure 9a, NO was introduced after the pre-adsorption of NH_3 for 2 h. The initial conversion of NO_x , NO , and NO_2 was 61%, 56%, and 97%, respectively. With a steady flow of NO_x , adsorbed ammonia was consumed gradually and the conversion of NO_x and NO decreased, while NO_2 conversion went down-up-down. According to the in situ DRIFTS results, it might be that NO_2 is easier to be adsorbed on the catalysts surface, thus leading to the decrease of NH_3 adsorption; the conversion of NO_2 dropped correspondingly. Until NH_3 was completely consumed, NO_2 started to be adsorbed on catalysts and the conversion went up, and decreased again after adsorption saturation. By feeding NH_3 and NO simultaneously, the conversion rate of NO_x and NO was lower than if only NO was fed, suggesting that NO_2 occupied active reaction sites resulting in its poor performance. In the case of feeding NH_3 and NO at the same time, we found that all the three conversion rates showed the same trend, namely, that the conversion rate reduced after the first rise, which is associated

with the promotion of NH_3 for SCR reaction. When the three gases: NH_3 ; NO ; and, O_2 were fed synchronously, the NO_x conversion rate reached a stable level of 80%. Simultaneously, the conversion rate of NO and NO_2 stabilized at 73% and 92%, respectively. What is more, both conversion rates obviously increased, indicating that NO_2 was easier to be reduced. We can conclude that O_2 was essential for the SCR reaction.

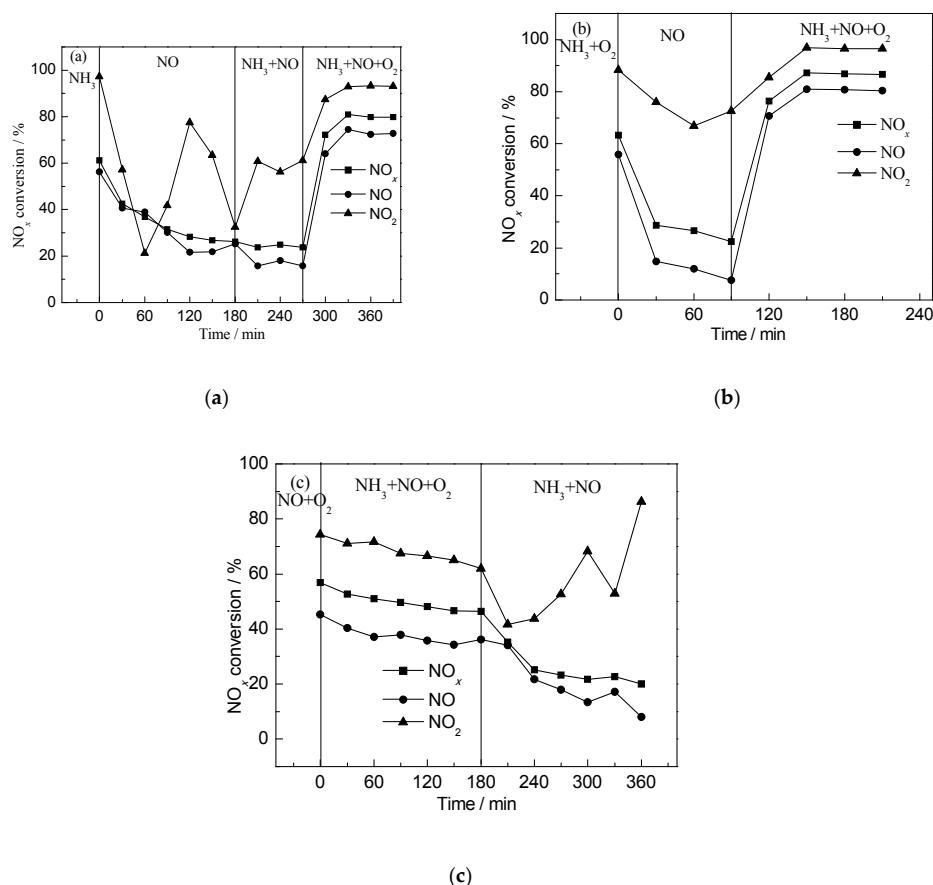


Figure 9. Transient SCR (selective catalytic reduction) activity tests (250 °C) under different pre-adsorption conditions: (a) pre-adsorption of NH_3 ; (b) pre-adsorbed of NH_3 and O_2 and (c) pre-adsorption of $\text{NO} + \text{O}_2$.

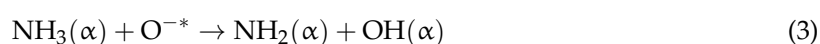
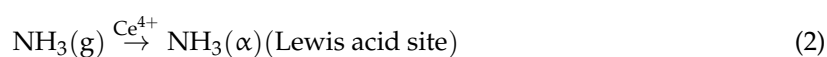
In Figure 9b, NO was introduced after NH_3 and O_2 was pre-adsorbed for 2 h. It was obvious that the conversion rate of NO_x reduced compared to Figure 9a. However, the conversion rate of NO_2 increased and the conversion rate of NO decreased. This might have been caused by the pre-adsorbed O_2 reacting with NO and producing NO_2 , which was easier to react with, and be adsorbed by, the catalysts. The conversion rate increased rapidly when NH_3 , NO , and O_2 was present at the same time.

In Figure 9c, after the pre-adsorption of $\text{NO} + \text{O}_2$ for 2 h, the denitration efficiency declined continuously with the existence of NH_3 , NO , and O_2 . When introducing NH_3 and NO together, the conversion rate of NO_x and NO went down-up-down, while the conversion rate of NO_2 went down-up-down-up. This could be ascribed to the oxygen storage-release capacity of CeO_2 . NO adsorbed on the catalysts, reacted with O_2 , and produced NO_2 , resulting in the ascended e-conversion rate of NO_2 . When O_2 was completely consumed, the conversion rate went down again. In this process, the SCR reaction was very weak. As a result, most of the NO_2 adsorbed on the catalysts, so its conversion rate went up. After this, O_2 reacted with NO and produced more NO_2 , and its conversion rate declined after the adsorption of NO_2 was saturated. When O_2 reacted with NO completely, NO_2 occupied the adsorption sites of O_2 , leading to the conversion rate going

up. The combined effect of the NO₂ and NO conversion rate resulted in the conversion of NO_x going down-up-down-up.

2.5. Low-Temperature SCR Reaction Pathway

The above analyses of in situ DRIFTS have demonstrated the relatively high ability of 1 wt. % V₂O₅-0.2CeO₂/TiO₂-ZrO₂ catalyst on NH₃ adsorption and oxidation. At the reaction temperature (250 °C), the Lewis acid sites were much more stable than were the Brønsted acid sites and the quantity of coordinated NH₃ was larger than that of the NH₄⁺ ions. The gaseous NH₃ was adsorbed on the catalytic surface, followed by a reaction with the gas phase NO to form the intermediate of NH₂NO, which was unstable and would decompose into N₂ and H₂O (Eley–Rideal mechanism). Based on the combination of in situ DRIFTS experiments and transient SCR activity tests, the mechanism of NH₃-SCR reaction over V₂O₅-CeO₂/TiO₂-ZrO₂ catalysts are mainly as followed:



3. Materials and Methods

3.1. Catalyst Preparation

The Ti-Zr support (molar ratio of Ti:Zr = 1:1) was prepared by a co-precipitation method. Typically, an equal molar amount of TiCl₄ solution and ZrOCl₂·8H₂O was dissolved in the deionized water. NH₃·H₂O solution was dropped into a stoichiometric solution of TiCl₄ and ZrOCl₂·8H₂O with steady stirring until the pH reached 10. The obtained precipitation solution was aged in air for 24h at room temperature, and then washed with deionized water until the supernatant was free from Cl⁻. Subsequently, the resulting paste was dried at 110 °C for 12 h and then calcined at 450 °C for 4 h in a muffle stove.

1 wt. % V₂O₅-0.2CeO₂/TiO₂-ZrO₂ samples were prepared by the step-by-step impregnation of Ti-Zr and CeNO₃·6H₂O (Ce/Ti = 0.2, molar ratio). The obtained mixture was stirred for 2 h at 25 °C, and then for about 4 h at 85 °C until the water boiled away. The resulting precipitate was dried at 110 °C for 12 h, followed by being calcined at 450 °C for 4 h in a muffle stove to obtain intermediate CeO₂/Ti-Zr, which was then impregnated with a NH₄VO₃ solution. The obtained mixture was dried and calcined in the same process of preparing CeO₂/Ti-Zr samples to finally acquire 1 wt. % V₂O₅-0.2CeO₂/TiO₂-ZrO₂ samples.

3.2. In situ DRIFTS Experiments

In situ DRIFTS investigations were carried out on a Nicolet 6700 spectrometer (Thermo Electron Corporation, Waltham, MA, USA), running in the wavenumber range of 400–4000 cm⁻¹ at a resolution of 4 cm⁻¹. A thin, intact and self-supporting wafer of adsorbents were prepared and mounted inside a high temperature cell (HTC-3, Harrick Scientific Corporation, Ithaca, NY, USA). Prior to each experiment, the catalyst was heated to 400 °C under an N₂ atmosphere for 1h to remove any adsorbed species, then cooled down to the reaction temperature. The background spectrum was recorded in N₂ flow and was automatically subtracted from the sample spectrum during the experiment. Then the N₂ flow was switched to a stream containing one or more reactants, such as NH₃, NO, and O₂. In situ DRIFTS experiments included transient response and steady-state response experiments. It should be noted that new catalyst samples pretreated under the same conditions and were used in each in situ DRIFTS experiments.

3.3. Transient SCR Activity Tests

As shown in Table 1, in order to coordinate the in situ DRIFTS experiments, catalyst activity test experiments were designed under different conditions of feeding gases. A total of 0.3 g of catalyst (screening through 40 to 60 mesh sieve) was tested on a fixed-bed quartz tube reactor (Nanjing University of Technology, Nanjing, China) with an internal diameter of 7 mm at the temperature of 250 °C. The total flow rate was 100 mL/min, which was pre-mixed in a gas mixer to obtain the simulated gas containing 0.08% NO, 0.08% NH₃, and 5% O₂, with a balance of N₂, NO, NO₂, and NO_x in the outlet, which was continually monitored by a flue gas analyzer (Testo 330-2 LL, Shanghai, China). Typically, during the experiments, about 5% NO was converted to NO₂. In other words, 5% NO_x existed in the form of NO₂.

Table 1. The working conditions of transient SCR activity tests.

Gas Composition	1	2	3	4
I	NH ₃	NO	NH ₃ + NO	NH ₃ + NO + O ₂
II	NH ₃ + O ₂	NO	NH ₃ + NO + O ₂	-
III	NO + O ₂	NH ₃ + NO + O ₂	NH ₃ + NO	-

4. Conclusions

In situ DRIFTS experiments and transient SCR activity tests were used coordinately to observe active and intermediate species and to describe the possible reaction path of 1 wt. % V₂O₅-0.2CeO₂/TiO₂-ZrO₂ at low temperature. The results are as followed:

- (1) NH₃ held a dominant position in the competitive adsorption between NH₃ and NO. Transient SCR activity tests showed that the NH₃ pre-adsorbed catalyst exhibited better SCR activity than its NO_x pre-adsorbed counterpart.
- (2) NO might be adsorbed on the catalyst surface and be converted to monodentate nitrite and nitrate species, which is more obvious in the presence of O₂, and dramatically restrains the adsorption of NH₃, hindering the SCR reaction.
- (3) More acid sites and reaction intermediate species -NH₂ at lower temperatures mainly led to the higher activity of the V₂O₅-0.2CeO₂/TiO₂-ZrO₂ catalyst.
- (4) Transient SCR activity tests and steady-state response experiments both confirmed that NH₃-SCR activity was enhanced by the presence of O₂. NH₃ adsorption intensity had no obvious difference, whether NO or O₂ was introduced or not, indicating that the adsorption and consumption of NH₃ was in dynamic equilibrium, which promoted SCR reaction.
- (5) NH₃-SCR reaction over 1 wt. % V₂O₅-0.2CeO₂/TiO₂-ZrO₂ catalyst mainly follows the E-R mechanism.

Author Contributions: S.K. and Y.Z. conceived and designed the experiments; X.Y. and T.H. performed the experiments; Y.Z. and B.L. analyzed the data and contributed reagents and materials; Y.Z. wrote the paper.

Funding: This work was supported by the Key Research and Development Projects of Jiangsu Province (BE2017716) and the National Key R&D Plan (2017YFB0603201).

Acknowledgments: This work was carried out in Key Laboratory of Energy Thermal Conversion and Control of Ministry of Education, based in Southeast University. The authors thank for the managers of the instruments in the laboratory.

Conflicts of Interest: The authors declare no conflicts of interest.

References

1. Nova, I.; Ciardelli, C.; Tronconi, E.; Chatterjee, D.; Bandlkonrad, B. NH₃-SCR of NO over a V-based catalyst: Low-T redox kinetics with NH₃ inhibition. *AIChE J.* **2006**, *52*, 3222. [[CrossRef](#)]
2. Xu, H.; Shen, Y.; Shao, C.; Lin, F.; Zhu, S.; Qiu, T. A novel catalyst of silicon cerium complex oxides for selective catalytic reduction of NO by NH₃. *J. Rare Earths* **2010**, *28*, 721–726. [[CrossRef](#)]

3. Topsoe, N.Y.; Dumesic, J.A.; Topsoe, H. Vanadia-titania catalysts for selective catalytic reduction of nitric-oxide by ammonia: I.I. Studies of active sites and formulation of catalytic cycles. *J. Catal.* **1995**, *151*, 241–252. [[CrossRef](#)]
4. Arnarson, L.; Falsig, H.; Rasmussen, S.B.; Lauritsen, J.V.; Moses, P.G. The reaction mechanism for the SCR process on monomer V⁵⁺ sites and the effect of modified Bronsted acidity. *Phys. Chem. Chem. Phys.* **2016**, *18*, 17071–17080. [[CrossRef](#)] [[PubMed](#)]
5. Marberger, A.; Ferri, D.; Elsener, M.; Krocher, O. The Significance of Lewis Acid Sites for the Selective Catalytic Reduction of Nitric Oxide on Vanadium-Based Catalysts. *Angew. Chem. Int. Ed.* **2016**, *128*, 11989–11994. [[CrossRef](#)] [[PubMed](#)]
6. Xiong, S.; Liao, Y.; Dang, H.; Qi, F.; Yang, S. Promotion mechanism of CeO₂ addition on the low temperature SCR reaction over MnO_x/TiO₂: A new insight from the kinetic study. *RSC Adv.* **2015**, *5*, 27785–27793. [[CrossRef](#)]
7. Vuong, T.H.; Radnik, J.; Rabeah, J.; Bentrup, U.; Schneider, M.; Atia, H.; Armbruster, U.; Grunert, W.; Bruckner, A. Efficient VO_x/Ce_{1-x}Ti_xO₂ catalysts for low-temperature NH₃-SCR: Reaction mechanism and active sites assessed by in situ/operando spectroscopy. *ACS Catal.* **2017**, *7*, 1693–1705. [[CrossRef](#)]
8. Zhang, T.; Qu, R.; Su, W.; Li, J. A novel Ce–Ta mixed oxide catalyst for the selective catalytic reduction of NO_x with NH₃. *Appl. Catal. B Environ.* **2015**, *176*, 338–346. [[CrossRef](#)]
9. Zhang, Y.; Zhu, X.; Shen, K.; Xu, H.; Sun, K.; Zhou, C. Influence of ceria modification on the properties of TiO₂–ZrO₂ supported V₂O₅ catalysts for selective catalytic reduction of NO by NH₃. *J. Colloid Interface Sci.* **2012**, *376*, 233–238. [[CrossRef](#)] [[PubMed](#)]
10. Liu, Z.; Zhu, J.; Li, J.; Ma, L.; Woo, S.I. Novel Mn–Ce–Ti Mixed-Oxide catalyst for the selective catalytic reduction of NO_x with NH₃. *ACS Appl. Mater. Interfaces* **2014**, *6*, 14500–14508. [[CrossRef](#)] [[PubMed](#)]
11. Zhang, L.; Pierce, J.; Leung, V.L.; Wang, D.; Epling, W.S. Characterization of ceria's interaction with NO_x and NH₃. *J. Phys. Chem. C* **2013**, *117*, 8282–8289. [[CrossRef](#)]
12. Galvez, M.E.; Boyano, A.; Lazaro, M.J.; Moliner, R. A study of the mechanisms of NO reduction over vanadium loaded activated carbon catalysts. *Chem. Eng. J.* **2008**, *144*, 10–20. [[CrossRef](#)]
13. Yu, J.; Si, Z.; Chen, L.; Wu, X.; Weng, D. Selective catalytic reduction of NO_x by ammonia over phosphate-containing Ce_{0.75}Zr_{0.25}O₂ solids. *Appl. Catal. B Environ.* **2015**, *163*, 223–232. [[CrossRef](#)]
14. Ma, Z.; Wu, X.; Si, Z.; Weng, D.; Ma, J.; Xu, T. Impacts of niobia loading on active sites and surface acidity in NbO_x/CeO₂–ZrO₂ NH₃–SCR catalysts. *Appl. Catal. B Environ.* **2015**, *179*, 380–394. [[CrossRef](#)]
15. Hu, H.; Zha, K.; Li, H.; Shi, L.; Zhang, D. In situ DRIFTS investigation of the reaction mechanism over MnO_x-MO_y/Ce_{0.75}Zr_{0.25}O₂ (M=Fe, Co, Ni, Cu) for the selective catalytic reduction of NO_x with NH₃. *Appl. Surf. Sci.* **2016**, *387*, 921–928. [[CrossRef](#)]
16. Zhang, Y.; Guo, W.; Wang, L.; Song, M.; Yang, L.; Shen, K.; Xu, H.; Zhou, C. Characterization and activity of V₂O₅-CeO₂/TiO₂-ZrO₂ catalysts for NH₃-selective catalytic reduction of NO_x. *Chin. J. Catal.* **2015**, *36*, 1701–1710. [[CrossRef](#)]
17. Underwood, G.M.; Miller, T.M.; Grassian, V.H. Transmission FT-IR and knudsen cell study of the heterogeneous reactivity of gaseous nitrogen dioxide on mineral oxide particles. *J. Phys. Chem. A* **1999**, *103*, 6184–6190. [[CrossRef](#)]
18. Ramis, G.; Angeles Larrubia, M. An FT-IR study of the adsorption and oxidation of N-containing compounds over Fe₂O₃/Al₂O₃ SCR catalysts. *J. Mol. Catal. A Chem.* **2004**, *215*, 161–167. [[CrossRef](#)]
19. Martínezarias, A.; Soria, J.; Conesa, J.C.; Seoane, X.L.; Arcoya, A.; Cataluna, R. NO reaction at surface oxygen vacancies generated in cerium oxide. *J. Chem. Soc. Faraday Trans.* **1995**, *91*, 1679–1687. [[CrossRef](#)]
20. Kijlstra, W.S.; Brands, D.S.; Poels, E.K.; Bliet, A. Mechanism of the selective catalytic reduction of NO by NH₃ over MnO_x/Al₂O₃.1. Adsorption and desorption of the single reaction components. *J. Catal.* **1997**, *171*, 208–218. [[CrossRef](#)]
21. Kijlstra, W.S.; Brands, D.S.; Smit, H.I.; Poels, E.K.; Bliet, A. Mechanism of the selective catalytic reduction of NO by NH₃ over MnO_x/Al₂O₃.2. Reactivity of adsorbed NH₃ and NO complexes. *J. Catal.* **1997**, *171*, 219–230. [[CrossRef](#)]
22. Hadjiivanov, K.; Knözinger, H. Species formed after NO adsorption and NO + O₂ co-adsorption on TiO₂: An FTIR spectroscopic study. *Phys. Chem. Chem. Phys.* **2000**, *2*, 2803–2806. [[CrossRef](#)]
23. Kantcheva, M. Identification, stability, and reactivity of NO_x species adsorbed on Titania-Supported manganese catalysts. *J. Catal.* **2001**, *204*, 479–494. [[CrossRef](#)]

24. Qi, G.; Yang, R.T.; Chang, R. MnO_x-CeO₂, mixed oxides prepared by co-precipitation for selective catalytic reduction of NO with NH₃ at low temperatures. *Appl. Catal. B Environ.* **2004**, *51*, 93–106. [[CrossRef](#)]
25. Long, R.Q.; Yang, R.T. Selective catalytic reduction of NO with Ammonia over Fe³⁺-Exchanged mordenite (Fe-MOR): Catalytic performance, characterization, and mechanistic Study. *J. Catal.* **2002**, *207*, 224–231. [[CrossRef](#)]
26. Guan, B.; Lin, H.; Zhu, L.; Huang, Z. Selective catalytic reduction of NO_x with NH₃ over Mn, Ce substitution Ti_{0.9}V_{0.1}O_{2-δ} nanocomposites catalysts prepared by self-propagating high-temperature synthesis method. *J. Phys. Chem. C* **2011**, *115*, 12850–12863. [[CrossRef](#)]
27. Jung, S.M.; Grange, P. Investigation of the promotional effect of V₂O₅ on the SCR reaction and its mechanism on hybrid catalyst with V₂O₅ and TiO₂-SO₄²⁻ catalysts. *Appl. Catal. B Environ.* **2002**, *36*, 207–215. [[CrossRef](#)]
28. Centeno, M.A.; Carrizosa, I.; Odriozola, J.A. In situ DRIFTS study of the SCR reaction of NO with NH₃ in the presence of O₂ over lanthanide doped V₂O₅/Al₂O₃ catalysts. *Appl. Catal. B Environ.* **1998**, *19*, 67–73. [[CrossRef](#)]
29. Chen, L.; Li, J.; Ge, M. DRIFT study on Cerium-Tungsten/Titania catalyst for selective catalytic reduction of NO_x with NH₃. *Environ. Sci. Technol.* **2010**, *44*, 9590–9596.



© 2018 by the authors. Licensee MDPI, Basel, Switzerland. This article is an open access article distributed under the terms and conditions of the Creative Commons Attribution (CC BY) license (<http://creativecommons.org/licenses/by/4.0/>).